Food & Function

PAPER

View Article Online
View Journal | View Issue

Cite this: *Food Funct.*, 2014, **5**, 2743

Complex coacervation with whey protein isolate and gum arabic for the microencapsulation of omega-3 rich tuna oil

Divya Eratte,[a] Bo Wang,[c] Kim Dowling,[a] Colin. J. Barrow[c] and Benu P. Adhikari*[b]

Tuna oil rich in omega-3 fatty acids was microencapsulated in whey protein isolate (WPI)–gum arabic (GA) complex coacervates, and subsequently dried using spray and freeze drying to produce solid microcapsules. The oxidative stability, oil microencapsulation efficiency, surface oil and morphology of these solid microcapsules were determined. The complex coacervation process between WPI and GA was optimised in terms of pH, and WPI-to-GA ratio, using zeta potential, turbidity, and morphology of the microcapsules. The optimum pH and WPI-to-GA ratio for complex coacervation was found to be 3.75 and 3 : 1, respectively. The spray dried solid microcapsules had better stability against oxidation, higher oil microencapsulation efficiency and lower surface oil content compared to the freeze dried microcapsules. The surface of the spray dried microcapsules did not show microscopic pores while the surface of the freeze dried microcapsules was more porous. This study suggests that solid microcapsules of omega-3 rich oils can be produced using WPI–GA complex coacervates followed by spray drying and these microcapsules can be quite stable against oxidation. These microcapsules can have many potential applications in the functional food and nutraceuticals industry.

Received 6th April 2014,
Accepted 29th June 2014

DOI: 10.1039/c4fo00296b

www.rsc.org/foodfunction

1. Introduction

The health benefits associated with the consumption of omega-3 fatty acids are well known, particularly for maintaining normal brain function,[1] reducing the risk of cancer[2] and preventing cardiovascular disease.[3] The lower actual *versus* recommended daily intake (RDI) of omega-3 fatty acids in many countries has been the major driving force for the development of functional foods and nutraceuticals containing eicosapentaenoic acid (EPA, C20:5n3) and docosahexaenoic acid (DHA, C22:6n3). Fish oil is the major source of EPA and DHA for fortified foods and nutritional supplements.[4,5] However, fish oils are highly susceptible to oxidation due to the highly unsaturated structure of long-chain omega-3 fatty acids. Oxidation of polyunsaturated fatty acids (PUFAs) produces peroxides and other harmful secondary oxidation products, which ultimately decreases the nutritional value of omega-3 fatty acids and negatively impacts the sensory properties.[6,7] Hence, the need for omega-3 rich oils to be microencapsulated in suitable wall materials to preserve their nutritional and organoleptic quality is ascertained.[8,9]

Complex coacervation is a liquid–liquid phase separation phenomenon that occurs when electrostatically opposite charged biopolymers are brought together under certain specific conditions.[10] Barrow *et al.*[11] reported that it is one of the most effective methods of microencapsulating omega-3 fatty acids rich oils, primarily using gelatine as the wall material. Broadening the range of suitable wall material for the microencapsulation of omega-3 fatty acids is important for expanding the scope and applicability of this important technique. Hence in the present study we explored the process of complex coacervate formation between cationic whey protein isolate and anionic gum arabic to microencapsulate tuna oil which is rich in omega-3 fatty acids. WPI is a by-product of the dairy industry and it has been widely used in the food processing industry due to its nutritional qualities and unique physiochemical properties such as emulsion stabilization and gel formation.[12] As a natural protein, WPI exhibits positive charge below its isoelectric point (IEP). WPI is effective in lowering interfacial tension at the oil–water interface, quite promptly migrates to the interface from bulk solution, and possesses good skin forming ability when it is dried.[13] GA is a composite edible polysaccharide which shows a negative charge above pH 2.2.[14] It is one of the most commonly used stabilizers in the food and pharmaceutical industries.[15] GA mainly consists of six carbohydrates moieties and less than 2% proteins.[16,17] Hence, complex coacervation between WPI and GA can occur by adjusting the pH and the WPI-to-GA ratio of their mixture.

[a]*School of Health Science, Federation University Australia, Mount Helen, VIC 3353, Australia*
[b]*School of Applied Science, RMIT, Melbourne, VIC 3001, Australia.*
E-mail: benu.adhikari@rmit.edu.au; Fax: +61 3 992 53747; Tel: +61 3 992 59940
[c]*Centre for Chemistry and Biotechnology, Deakin University, Geelong, VIC 3217, Australia*

However, there are only limited studies on the microencapsulation of oils using WPI–GA complex coacervates. Weinbreck *et al.*[18] encapsulated sunflower oil, lemon and orange oil flavours with WPI–GA coacervates. However, this work did not proceed to produce dried microcapsules and was confined in producing liquid microcapsules. Zhang *et al.*[19] investigated the encapsulation of fish oil using WPI–GA complex coacervates. This work focussed mainly on studying the effect of different GA and WPI types in forming complex coacervates and microcapsules. So far, the optimization of complex coacervation process between WPI and GA aiming to better microencapsulate omega-3 rich oils has not been systematically studied.

Dried microcapsules produced through complex coacervation could offer omega-3 rich oils better shelf-life and wider applicability.[20] Both spray and freeze drying are commonly used in the food industry to produce powder or solid microcapsules. However, the application of different drying techniques can influence the stability and other characteristics of powdered microcapsules even at the same optimal complexation and emulsification conditions. For example, the freeze dried products are more porous due to the sublimation while spray dried powders containing biopolymers are usually irregular and contain surface folds.[21,22] However, the effect of spray and freeze drying processes on the microencapsulation efficiency, surface oil and oxidative stability of solid microcapsules produced using WPI–GA complex coacervates is poorly understood.

In this context, there were three key objectives in this study. Firstly, to determine the optimum process parameters at which complex coacervation between WPI and GA can occur. Secondly, to produce and characterise the liquid microcapsules of omega-3 rich tuna oil produced by using these WPI–GA complex coacervates as the shell of the microcapsules. Finally, to produce and characterise spray and freeze dried solid microcapsules in terms of oxidative stability, microencapsulation efficiency, and surface oil content and morphological analysis through scanning electron microscopic (SEM) examinations.

2. Materials and methods

2.1 Materials

Whey protein isolate (WPI 895™) was donated by Fonterra Cooperative, New Zealand. Gum arabic was purchased from Sigma-Aldrich Ltd (New South Wales, Australia). Tuna oil (HiDHA), containing 39.03% omega-3 fatty acids (Table 1), was a gift from NuMega Ingredients Ltd. (Victoria, Australia) and stored at 4 °C until use. All other chemicals were purchased from Sigma-Aldrich Australia (New South Wales, Australia) and were of analytical grade and used without further purification.

Table 1 Omega-3 fatty acids composition of tuna oil[a]

Omega-3 fatty acids	Percentage (%)
16:3w3	0.97
18:3w3 ALA	0.40
18:4w3	0.60
20:4w3	0.46
20:5w3 EPA	5.98
22:5w3	1.20
22:6w3 DHA	29.42
Sum omega-3–PUFAS	39.03

[a] NuMega Ingredients Ltd. (Victoria, Australia).

2.2 Optimization of the complex coacervation process

The zeta potential, yield of complex coacervates and turbidity data were used to determine the optimum pH and WPI-to-GA ratio for the formation of complex coacervates.

2.2.1 Optimization of pH. Zeta potential values as a function of pH were used to determine the optimal pH range at which complex coacervation between WPI and GA was formed. Zeta potential values for WPI (1.5% w/w) and GA (0.5% w/w) were measured in the pH range of 3.0–7.0 at 25 °C by using a zetasizer (Zetasizer NanoZS 90, Malvern Instruments Ltd. Worcestershire, WR14 1XZ, UK), which determines the electrophoretic mobility and then calculates the zeta potential using appropriate conversion equations.[23,24]

The absorbance of the mixture of WPI (0.1%) and GA (0.03%) was measured within 3.0–5.0 pH range using a UV spectrophotometer (UV-1800, Shimadzu, Kyoto, Japan) at 750 nm. The absorbance (or turbidity) of WPI (0.1%, w/w), GA (0.03%, w/w), and the mixture of WPI and GA at different ratios, were measured at 750 nm. The pH value at which the maximum absorbance (turbidity) was observed was considered the optimal pH for complex coacervation between WPI and GA.

2.2.2 Optimization of the WPI-to-GA ratio. The turbidities of various mixtures of WPI and GA at different ratios (1 : 1, 3 : 1, 3 : 2, 4 : 1 and 5 : 1) were determined using the light absorbance of these mixtures at 750 nm using a UV spectrophotometer as detailed above.

The optimum WPI-to-GA ratio which resulted in the highest coacervation yield was also measured. For this purpose, aqueous dispersions containing WPI and GA at the above mentioned ratios were prepared at ambient temperature and the pH of these dispersions was adjusted to the optimum value (Section 2.2.1). These pH adjusted dispersions were allowed to stand for 5 h to facilitate the precipitation of the gel-like complex coacervates. Then, the coacervates were carefully separated and dried at 105 °C until a constant mass was reached. The coacervate yield was then calculated by using eqn (1) given below.

$$\text{Coacervate yield (\%)} = \frac{\text{Mass of the dried coacervates (g)}}{\text{Total mass of WPI + GA used (g)}} \quad (1)$$

2.3 Confocal laser scanning microscopic (CLSM) analysis

The microstructure of tuna oil microencapsulated with WPI–GA using complex coacervation at various pH was observed using a CLSM (Eclipse Ti, Nikon, Japan). WPI and GA were covalently labelled with fluorescein 5-isothiocyanate (FITC) and rhodamine B-isothiocyanate (RITC), respectively. Tuna oil was physically labelled with Bodipy-X-Azide. Briefly, FITC solution (10 mg per 100 ml ethanol) and RITC solution (10 mg per 100 ml water) were prepared separately. Then 50 ml of FITC solution and 50 ml of RITC solution were used for the preparation of WPI (3%) and GA (1%) solutions and the

microencapsulation procedure was carried out as per Section 2.4. Covalent labelling of WPI and GA was done in order to visualize these biopolymers in the mixture. A lens with 40× magnification and a laser with an excitation wavelength of 645 nm (for Bodipy-X-Azide), 488 nm (for FITC) and 561 nm (for RITC) were used.

2.4 Microencapsulation of tuna oil

Firstly, 250 ml WPI solution (3%, w/w) was prepared at ambient temperature and 15 g of tuna oil was dispersed in this solution. The mixture was stirred using a mechanical stirrer (IKA® RW 20 digital overhead stirrer, Germany) at 800 rpm for 10 min and was further homogenized using a microfluidizer at 45 MPa for 3 passes (M110L, Microfluidics, Newton, USA) to produce an O/W emulsion. Then 250 ml GA solution (1%, w/w) was added drop wise into this O/W emulsion and was stirred at 800 rpm. The pH of this emulsion was then adjusted to 3.75 by adding 1% citric acid drop wise in order to induce electrostatic interaction between WPI and GA. The microencapsulation procedure was carried out at 25 °C, followed by cooling to 5 °C at a rate of 5 °C h^{-1} using a programmable water bath (PolyScience, Niles, Illinois, USA). A microscope (Eclipse 80 i, Nikon, Japan) was used to obtain optical images of the coacervates microcapsules. The morphology of the microcapsules was captured as a function of pH and temperature. Finally, the microcapsules were dried to produce solid or powder microcapsules.

2.5 Drying of coacervate microcapsules

A portion of suspension containing microcapsules produced as per Section 2.4 was spray dried (Mini spray dryer B-290, BÜCHI Labortechnik, Switzerland) using inlet and outlet temperatures of 180 °C and 80 ± 3 °C, respectively. The powdered microcapsules were collected and stored in an air tight desiccator for further characterization.

The second portion of the liquid microcapsules was frozen at −20 °C overnight and was freeze dried (Christ Alpha 2-4LD, Osterode, Germany). The temperature of the ice condenser was set at −50 °C and the vacuum pressure was set to 0.04 mbar. The frozen samples were dried for 30 h and the dried product was collected, pulverized and stored in an air tight desiccator for further tests.

2.6 Physicochemical properties of the microcapsules

2.6.1 Oxidative stability. Accelerated oxidation tests were carried out for the liquid oil and the solid or powdered microcapsules using a Rancimat (model 743, Metrohm, Herisau, Switzerland).[25] Four ml tuna oil or 1.5 g dried microcapsule powder was heated at 90 °C under purified air (flow rate of 20 l h^{-1}). Briefly, when the oxidation of oil takes place, the conductivity of Milli-Q water in the collection chamber increases due to the entrapment of the volatile products (formic acid) and this increase is plotted by the accompanied software (Rancimat Control, version 1.1, Metrohm, Herisau, Switzerland). Then the OSI value of the samples is graphically determined by locating tangential intersection point on experimental data as described by Läubli *et al.*, 1986.[26] The induction time (at which the conductivity of sample increases sharply due to oxidation) of the test sample was recorded and used as the oxidative stability index (OSI). Analyses were performed in duplicate.

2.6.2 Microencapsulation efficiency. Microencapsulation efficiency was calculated by measuring the surface oil (solvent extractable) and total oil of the microcapsules. Surface oil was determined by the washing method described by Liu *et al.*[27] with slight modification. Three grams of dried microcapsule sample was dispersed in 30 ml isohexane and this was shaken at 225 rpm for 5 minutes on an orbital shaker (Stuart SSL-1, Carl Roth, Karlsruhe, Germany). The slurry was then filtered through filter paper (Whatman, 5 μm) and the solid particles caught on the filter were further washed three times with 10 ml of isohexane in each wash. The filtrate was dried under nitrogen followed by drying at 100 °C for 1 h in an oven. The sample dried in this way was placed in a fume hood overnight to remove the residual solvent. The surface oil content was then measured gravimetrically.

The total oil content in the dried microcapsules was determined by an acid digestion method using 4 N HCl. Three grams of powdered microcapsule sample was dispersed in 30 ml of 4 N HCl and shaken at 225 rpm for 15 minutes on an orbital shaker (Stuart SSL-1, Carl Roth, Karlsruhe, Germany) in order to dissolve the shell materials. Fifteen ml of isohexane was added to this mixture and then shaken for 18 h at ambient temperature to extract the oil. The mixture was centrifuged at 24 471*g* at 20 °C for 30 minutes. The hexane phase containing the dissolved oil was collected and dried by nitrogen under fume hood. This partially dried sample was further dried at 100 °C in an oven and then placed under a fume hood to remove the residual solvent. The oil content was then determined gravimetrically.

The percent surface oil (SO), total oil (TO) and microencapsulation efficiency (ME) were calculated using eqn (2)–(4), respectively.

$$\mathrm{SO} = \frac{w_s}{w_m} \times 100\% \quad (2)$$

$$\mathrm{TO} = \frac{w_t}{w_m} \times 100\% \quad (3)$$

$$\mathrm{ME} = \frac{w_t - w_s}{w_t} \times 100\% \quad (4)$$

where w_t and w_s are the mass values (g) of total and surface oil of the microcapsules and w_m is the mass (g) of the microcapsules.

2.7 Surface morphology of the solid microcapsules

A Scanning Electron Microscopy (JEOL JSM6300 SEM, Tokyo, Japan) was used to acquire the morphology of dried microcapsules. Samples were lightly gold sputter coated (Sputter coater, Agar Aids, England) for 45 seconds and imaged under scanning electron microscope operated at 7 kV and low beam current.

2.8 Statistical analysis

All measurements were performed at least in triplicates and the results are reported as mean ± standard deviation.

The SPSS statistical package (Version 21, Lead Technologies, USA) was used for the analysis of variance (ANOVA) to determine whether or not significant difference existed between two mean values. The confidence level of 95% ($p < 0.05$) was used.

3. Results and discussion

3.1 Optimal parameters for complex coacervation between WPI and GA

3.1.1 Optimal pH for complex coacervation. The zeta potentials of WPI and GA within the pH range of 3.0–7.0 are presented in Fig. 1A. The zeta potentials of WPI within this pH range varied from positive (16.80 mV at pH 3.0) to negative (−20.21 mV at pH 7.0). The isoelectric point (IEP) at which the zeta potential becomes zero was found to be 4.4, which is in agreement with previous reports.[28] The zeta potential of GA is always negative independently of pH due to carboxylate groups being the only charged functionalities present in its globular-like random coil structure.[29] If at least one of the macromolecules in a mixture is not a strong polyelectrolyte, then coacervation is likely to occur.[30] Therefore, it can be inferred from the Fig. 1A that the pH at which complex coacervation between WPI and GA will occur is at or below pH 4.4.

The turbidity test (Section 2.2.1) was carried out within the pH range of 3.0–5.0 in order to locate the optimum pH value for complex coacervate formation. The absorbance values of the WPI and GA mixed dispersions are presented in Fig. 1B. As can be seen from this figure, formation of dense complex coacervates occurred within the pH range and formation of the complex coacervates was greatest at pH 3.75. Hence this pH value was chosen as the optimum pH for complex coacervate formation.

3.1.2 Optimal WPI-to-GA ratio for complex coacervation. The ratio of protein to polysaccharide in the mixture influences the charge balance of polyions and consequently their complexation behaviour.[31] Based on the work described in the previous section (Section 3.1.1) we used the optimum pH of 3.75 to study the binding between WPI and GA. As can be seen from Fig. 2A, the highest absorbance value was observed at a WPI-to-GA ratio of 3 : 1, which is due to the highest level of turbidity caused by the electrostatic interaction between WPI and GA. To corroborate this data, the yield of complex coacervates was measured (Section 2.2.2) at different WPI-to-GA ratios and the data is presented in Fig. 2B. The highest coacervate yield of 71.26% was obtained at the WPI-to-GA ratio of 3 : 1, which corroborates the turbidity data (Fig. 2A). Other WPI-to-GA ratios produced lower coacervate yields, possibly due to the formation of soluble rather than insoluble complexes occurring when either of the biopolymer is in excess. Soluble complexes are formed due to the charge imbalance and produce weaker electrostatic interaction, which results in lower coacervate yield.[31] The biopolymer ratio and dispersion pH are known to alter the charge density of the complexes.[23] At pH 3.75 and WPI-to-GA ratio of 3 : 1, the electrostatic interaction between WPI and GA resulted in two phases specifically due to the

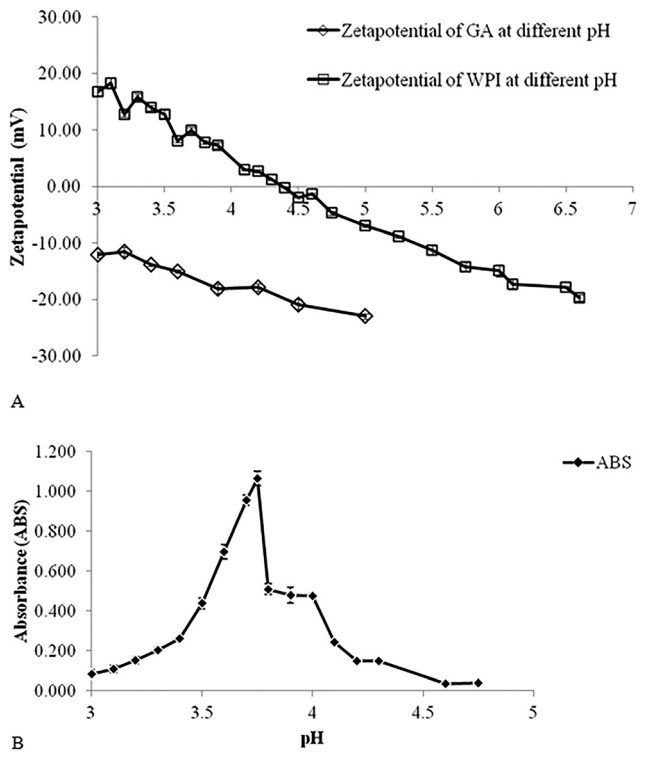

Fig. 1 (A) Effect of pH on zeta potential of WPI and GA dispersions. (B) Turbidity values of WPI and GA mixed dispersions at different pH values at WPI to GA ratio = 3 : 1.

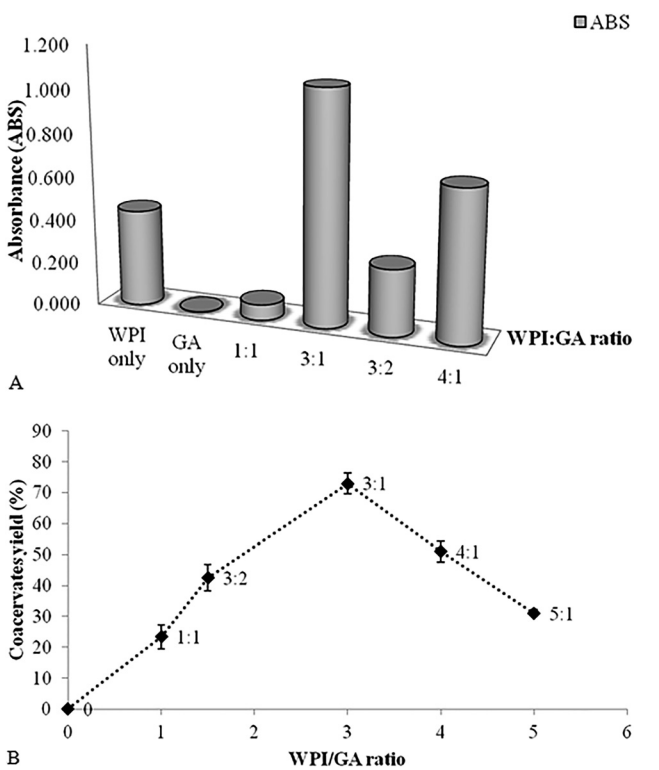

Fig. 2 (A) Turbidity values at different WPI to GA ratios. (B) Yield of complex coacervates at different WPI to GA ratios.

formation of a soft dense coacervate phase rich in biopolymers and a dilute phase poor in biopolymer concentrations. Hence, this WPI-to-GA ratio of 3 : 1 was selected as the optimum ratio to produce complex coacervates.

3.2 Observation of microcapsule formation

Optical microscopy was used to study the formation of complex coacervates and their subsequent absorption onto oil droplets. As can be seen from Fig. 3A–C, no obvious complex coacervates were absorbed onto the oil droplets above pH 5.0. When the pH was further lowered to 4.5 (close to the IEP of WPI), the aggregation of oil droplets was observed (Fig. 3D). This may be due to weaker repulsion between negatively charged WPI and GA when the surface charge of WPI approaches neutral (Fig. 1A). Also, the steric repulsion between droplets was not enough to overcome the aggregation of the droplets. In this environment, the attractive interactions between the biopolymer molecules, such as van der Waals and hydrophobic, become dominant. Kulmyrzaev *et al.*[32] reported that excessive droplet aggregation occurs when the net charge on the droplet doesn't generate stronger electrostatic repulsive force than the strength of the attractive forces in the emulsion. It can be observed from Fig. 3E to H that when the pH of the dispersion was lowered below the isoelectric point of WPI (IEP = 4.4), complex coacervation occurred in the surrounding continuous phase, and these coacervates migrated to the surface of the oil droplets, and formed a coacervates layer. It was observed that complex coacervation occurred and aggregation of the oil droplets started to take place below pH 4.4. This is because WPI became positively charged below its IEP and electrostatic attraction with negatively charged GA started to occur. Finally, a smooth layer of WPI–GA complex coacervates was formed uniformly around the oil droplets (Fig. 3G) at pH 3.75, which is consistent with the turbidity and coacervate yield data (Fig. 1B and 2A and B).

When the liquid microcapsules were cooled from ambient temperature to 5 °C, the "free coacervates" which remained suspended in the continuous phase (at ambient temperature) began to absorb onto the surface of the aggregated oil droplets (Fig. 3H). This implies that cooling is an important step in stabilizing oil emulsions using complex coacervates. As can be seen from Fig. 3H, multicored microcapsules were formed due to the formation of WPI–GA complex coacervates. This may be partly due to homogenization occurring under high pressure when using a microfluidizer. Yeo *et al.*[33] reported that single core microcapsules were produced when a lower degree of homogenization was used while multi core microcapsules were produced under a higher degree of homogenization.

Confocal laser scanning microscopy (CLSM) was used to visualize complex coacervate formation between WPI and GA and to confirm the optimized processing conditions (pH 3.75 and WPI-to-GA ratio 3 : 1) and also to assess whether tuna oil droplets were microencapsulated in the WPI–GA complex coacervates. WPI (labelled green) and GA (labelled red) in the dispersion before complex coacervation are shown in Fig. 4A and B. These figures are similar to the optical micrographs of dispersion before complex coacervation (Fig. 3A). WPI and GA are clearly visible in the complex coacervate as shown in Fig. 4C and D, respectively. The micrograph presented in Fig. 4C is WPI–GA complex coacervate (labelled WPI (green) only) formed under the optimized processing conditions. Similarly,

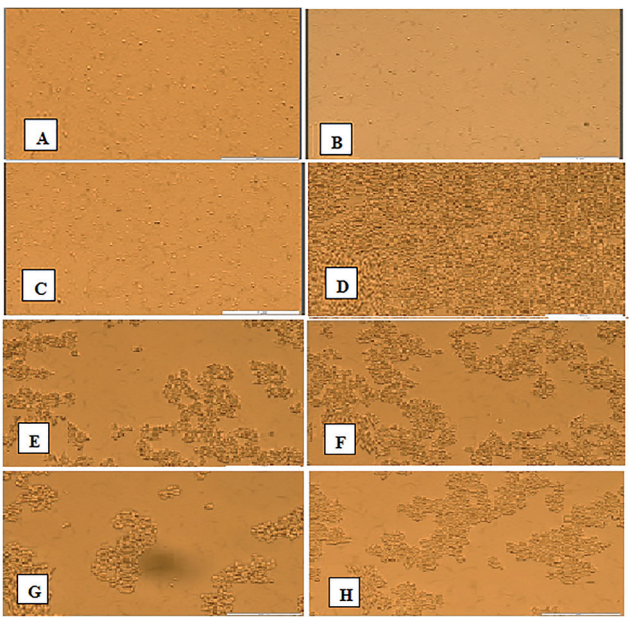

Fig. 3 WPI–GA complex coacervates observed through light microscopy as a function of pH. (A) pH 6.0; (B) pH 5.5; (C) pH 5.0; (D) pH 4.5; (E) pH 4.0; (F) pH 3.8; (G) pH 3.75 and (H) pH 3.75 after cooling, scale bar = 10 μm.

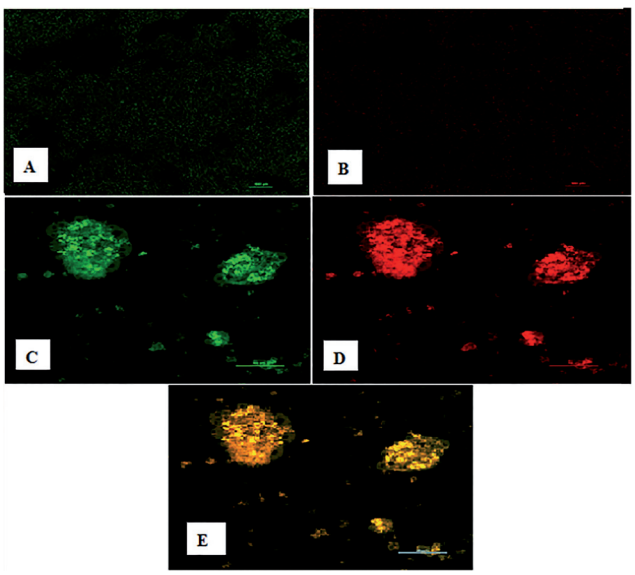

Fig. 4 Confocal scanning laser micrographs of (A) WPI (green) in the dispersion before carrying out complex coacervation at pH 6.0, (B) GA (red) in the dispersion before carrying out complex coacervation at pH 6.0 (C) complex coacervate with labelled WPI (green) at pH 3.75, (D) complex coacervate with labelled GA (red) at pH 3.75 and (E) complex coacervates of WPI and GA formed (yellow) at pH 3.75.

Fig. 4D is the WPI–GA complex coacervate (labelled GA (red) only) formed under the same optimized conditions. Fig. 4E shows that WPI–GA complex coacervate (yellow in colour) was formed at pH 3.75 and at a WPI-to-GA ratio of 3 : 1, and neither WPI (green colour) nor GA (red colour) is dominant in Fig. 4E, indicating that complex coacervation has occurred between WPI and GA under the processing conditions used. These CLSM images are consistent with the optimum conditions for formation of complex coacervates between WPI and GA being pH 3.75 and a WPI-to-GA ratio of 3 : 1.

Multiple labelling CLSM was used to visualize the distribution of tuna oil droplets (labelled blue) in the WPI–GA microcapsules (Fig. 5). Microcapsules without and with visualisation of oil droplets are shown in Fig. 5E and F, respectively, to assess whether complexation has occurred between WPI and GA at pH 3.75 and at the WPI-to-GA ratio of 3 : 1, and also to confirm the distribution of oil droplets in the microcapsules. The GA component in the microcapsule is shown in Fig. 5A (GA labelled red), the WPI component in Fig. 5B (WPI labelled green), and oil in Fig. 5C (oil droplets labelled blue). The mixture of oil, WPI and GA in the dispersion before carrying out complex coacervation process is presented in Fig. 5D. It can be clearly seen from Fig. 5D that no complex coacervates of WPI and GA was formed and oil droplets were just dispersed in the mixture at pH 6.0. An obvious formation of WPI–GA complex coacervate (yellow) and distribution of oil droplets in the coacervate can be clearly seen in Fig. 5E and F. The *Z*-average size of the oil droplets was 223.0 nm (polydispersity index (PdI) = 0.376) and these oil droplets are clearly microencapsulated in the WPI–GA matrix.

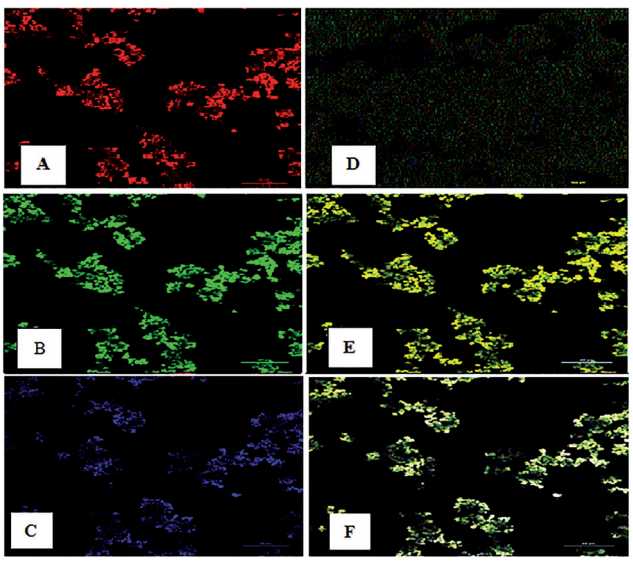

Fig. 5 Confocal scanning laser micrographs of (A) GA in the coacervate microcapsules (red), (B) WPI in the coacervate microcapsules (green), (C) oil droplets in the coacervate microcapsules (blue), (D) mixture of WPI (green), GA (red), and oil (blue) before carrying out complex coacervation at pH 6.0, (E) coacervate microcapsules not showing (blue) oil droplets at pH 3.75 and (F) coacervate microcapsules showing (blue) oil droplets at pH 3.75.

3.3 Effect of drying methods on the physiochemical characteristics of the microcapsules

Physiochemical properties (oxidative stability, surface oil, total oil, microencapsulation efficiency and morphological analysis through SEM) of spray and freeze dried tuna oil microcapsules produced by microencapsulating with WPI–GA complex coacervates are discussed in this section.

The OSI values of blank tuna oil (control), freeze dried and spray dried solid microcapsules are presented in Fig. 6. These OSI data suggest that both freeze and spray dried tuna oil microcapsules exhibited significantly ($p < 0.05$) better oxidative stability compared to the control (OSI = 3.1 h). The OSI value for freeze dried sample was 13.2 h compared to 22.1 h for spray dried sample implying that the freeze dried microcapsules were less stable against oxidation compared to the spray dried ones. This may be due to the highly porous structure of the freeze dried powder.[34] The porous structure makes it easier for oxygen to diffuse through the porous shell structure to access the encapsulated oil and weakens the oxidative stability.[35,36] This relatively poor oxidative stability in freeze dried microcapsules can also be explained by their morphology identified by SEM (Fig. 7B). Freeze dried microcapsules possess irregular shape, are flake-like and have a highly porous structure.

The spray dried microcapsules were found to be significantly more stable ($p < 0.05$) against oxidation, as compared to freeze dried microcapsules, even though much higher temperature was used in the spray drying process. This relatively high OSI of spray dried microcapsules can be attributed to the compact structure of the spray dried solid microcapsules (Fig. 7A). The outer topography of the spray dried particles indicates that there is no shell rupture and the shell is much less porous compared to freeze dried microcapsules. The absence of pores/cracks on the particle surface is very important for preventing the inward diffusion of oxygen and hence for better protection of the encapsulated oil. The SEM micrograph shows that the spray dried microcapsules have uniform size distribution below 5 μm (based on 100 microcapsules) with wrinkled spherical shape, resulting from the protein in

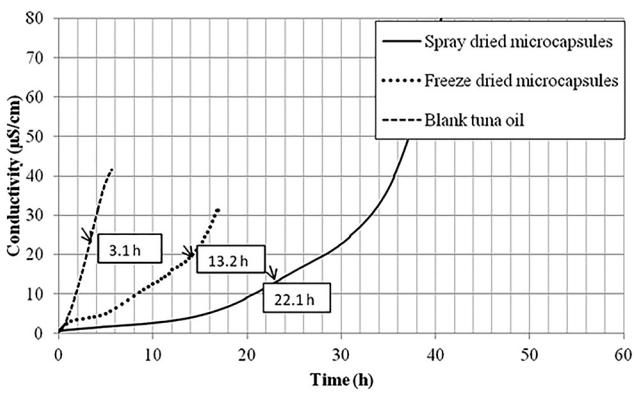

Fig. 6 Oxidative stability index of microcapsules measured by accelerated oxidation test using Rancimat™.

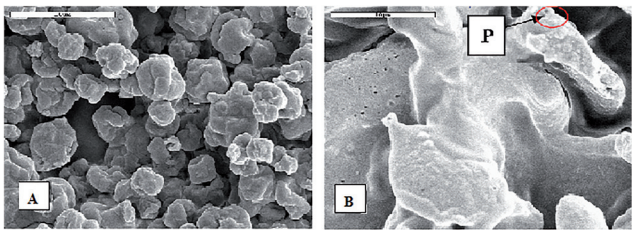

Fig. 7 SEM micrographs of spray dried (A) and freeze dried microcapsules (B). P indicates pores in the shell.

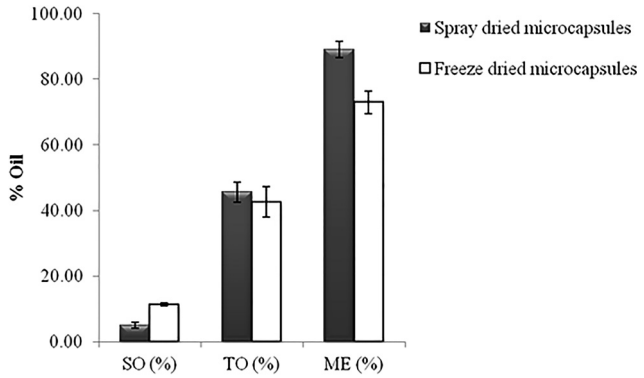

Fig. 8 Surface oil (SO), total oil (TO) and microencapsulation efficiency (ME) of spray dried and freeze dried complex coacervate microcapsules.

the wall material. The wrinkled surface is typical characteristics of spray dried powders with protein in the matrix.[37–39] Moreover, this significantly enhanced oxidative stability for spray dried microcapsules compared to freeze dried ones is partly due to lower overall surface area and lower surface oil content.

The surface oil and total oil contents, and microencapsulation efficiency of the freeze and spray dried microcapsules, are shown in Fig. 8. The freeze dried solid microcapsules had higher surface oil content (11.41%) as shown in Fig. 8, and lower microencapsulation efficiency. Surface oil is the unencapsulated oil found on the surface of the microparticles, and can trigger lipid oxidation and is a result of lower oil encapsulation efficiency.[40] The microencapsulation efficiency of freeze dried microcapsules was 72.95%, which is significantly ($p < 0.05$) lower than that of spray dried microcapsules (Fig. 8). Similar result was also observed by Quispe-Condori *et al.*[41] when investigating the microencapsulation efficiency of freeze dried and spray dried flaxseed oil microcapsules.

4. Conclusions

The complex coacervation process between WPI and GA was optimised in terms of pH and WPI-to-GA ratio. The WPI–GA complex coacervates were used to microencapsulate omega-3 rich tuna oil. Solid microcapsules of tuna oil were produced through spray drying and freeze drying. The optimal complexation pH and WPI-to-GA ratio were found to be 3.75 and 3 : 1, respectively. The spray dried microcapsules were found to be more stable against oxidation compared to those prepared by freeze drying. The spray dried microcapsules had the advantage of higher microencapsulation efficiency and lower surface oil content compared to the freeze dried samples. We conclude that WPI–GA complex coacervates can effectively microencapsulate omega-3 rich oils such as tuna oil and the solid microcapsules produced using spray drying will have high encapsulation efficiency and stability against oxidation.

Acknowledgements

The first author acknowledges the Australian Postgraduate Award (APA) provided to her by the Australian Federal Government. The authors wish to thank Bruce Armstrong Stafford McKnight, Alexander Nield, and Indrajeetsinh Rana for technical help during experiments. This work was partially supported by Australian Government's Collaborative Research Network (CRN) initiative.

References

1 R. K. McNamara and S. E. Carlson, *Prostaglandins, Leukotrienes Essent. Fatty Acids*, 2006, **75**, 329–349.
2 D. P. Rose and J. M. Connolly, *Pharmacol. Ther.*, 1999, **83**, 217–244.
3 H. C. Bucher, P. Hengstler, C. Schindler and G. Meier, *Am. J. Med.*, 2002, **112**, 298–304.
4 P. M. Kris-Etherton, W. S. Harris and L. J. Appel, *Arterioscler., Thromb., Vasc. Biol.*, 2003, **23**, e20–e30.
5 T. K. Dey, S. Ghosh, M. Ghosh, H. Koley and P. Dhar, *Food Res. Int.*, 2012, **49**, 72–79.
6 R. J. Hsieh and J. E. Kinsella, *Adv. Food Nutr. Res.*, 1989, **33**, 233–341.
7 E. N. Frankel, *Chem. Phys. Lipids*, 1987, **44**, 73–85.
8 K. Heinzelmann and K. Franke, *Colloids Surf., B*, 1999, **12**, 223–229.
9 J. Velasco, C. Dobarganes and G. Márquez-Ruiz, *Grasas Aceites*, 2003, **54**, 304–314.
10 V. Ducel, J. Richard, P. Saulnier, Y. Popineau and F. Boury, *Colloids Surf., A*, 2004, **232**, 239–247.
11 C. J. Barrow, C. Nolan and Y. Jin, *Lipid Technol.*, 2007, **19**, 108–111.
12 J. N. de Wit, *J. Dairy Sci.*, 1998, **81**, 597–608.
13 B. Adhikari, T. Howes, A. K. Shrestha and B. R. Bhandari, *Chem. Eng. Process.*, 2007, **46**, 420–428.
14 C. Butstraen and F. Salaün, *Carbohydr. Polym.*, 2014, **99**, 608–616.
15 S. Nie, C. Wang, S. W. Cui, Q. Wang, M. Xie and G. O. Phillips, *Food Hydrocolloids*, 2013, **31**, 42–48.
16 A. M. Islam, G. O. Phillips, A. Sljivo, M. J. Snowden and P. A. Williams, *Food Hydrocolloids*, 1997, **11**, 493–505.
17 N. Garti and M. E. Leser, *Polym. Adv. Technol.*, 2001, **12**, 123–135.

18 F. Weinbreck, M. Minor and C. De Kruif, *J. Microencapsulation*, 2004, **21**, 667–679.
19 W. Zhang, C. Yan, J. May and C. J. Barrow, *Agro Food Ind. Hi-Tech*, 2009, **20**, 18–21.
20 S. Ponsart and D. J. Burgess, *Eur. J. Pharm. Sci.*, 1996, **4**, 76.
21 C. Anandharamakrishnan, C. D. Rielly and A. G. Stapley, *Dairy Sci. Technol.*, 2010, **90**, 321–334.
22 A. Gharsallaoui, G. Roudaut, O. Chambin, A. Voilley and R. Saurel, *Food Res. Int.*, 2007, **40**, 1107–1121.
23 H. Espinosa-Andrews, K. E. Enríquez-Ramírez, E. García-Márquez, C. Ramírez-Santiago, C. Lobato-Calleros and J. Vernon-Carter, *Carbohydr. Polym.*, 2013, **95**, 161–166.
24 Y. Yuan, Z. Wan, X. Yang and S. Yin, *Food Res. Int.*, 2014, **55**, 207–214.
25 B. W. Mathäus, *J. Am. Oil Chem. Soc.*, 1996, **73**, 1039–1043.
26 M. W. Läubli and P. A. Bruttel, *J. Am. Oil Chem. Soc.*, 1986, **63**, 792–795.
27 S. Liu, N. Low and M. T. Nickerson, *J. Am. Oil Chem. Soc.*, 2010, **87**, 809–815.
28 B. Chen, H. Li, Y. Ding and H. Suo, *LWT–Food Sci. Technol.*, 2012, **47**, 31–38.
29 E. Dickinson, *Food Hydrocolloids*, 2003, **17**, 25–39.
30 C. G. de Kruif, F. Weinbreck and R. de Vries, *Curr. Opin. Colloid Interface Sci.*, 2004, **9**, 340–349.
31 A. Ye, *Int. J. Food Sci. Technol.*, 2008, **43**, 406–415.
32 A. Kulmyrzaev, M. P. C. Sivestre and D. J. McClements, *Food Res. Int.*, 2000, **33**, 21–25.
33 Y. Yeo, E. Bellas, W. Firestone, R. Langer and D. S. Kohane, *J. Agric. Food Chem.*, 2005, **53**, 7518–7525.
34 S. S. Sablani, M. S. Rahman, M. K. Al-Kuseibi, N. A. Al-Habsi, R. H. Al-Belushi, I. Al-Marhubi and I. S. Al-Amri, *J. Food Eng.*, 2007, **80**, 68–79.
35 M. S. Rahman, O. S. Al-Amri and I. M. Al-Bulushi, *J. Food Eng.*, 2002, **53**, 301–313.
36 P. N. Ezhilarasi, D. Indrani, B. S. Jena and C. Anandharamakrishnan, *J. Food Eng.*, 2013, **117**, 513–520.
37 A. Soottitantawat, F. Bigeard, H. Yoshii, T. Furuta, M. Ohkawara and P. Linko, *Innovative Food Sci. Emerging Technol.*, 2005, **6**, 107–114.
38 R. V. Tonon, C. R. F. Grosso and M. D. Hubinger, *Food Res. Int.*, 2011, **44**, 282–289.
39 Y. Y. Xu, T. Howes, B. Adhikari and B. Bhandari, *Drying Technol.*, 2013, **31**, 1939–1950.
40 N. Hardas, S. Danviriyakul, J. L. Foley, W. W. Nawar and P. Chinachoti, *LWT–Food Sci. Technol.*, 2000, **33**, 506–513.
41 S. Quispe-Condori, M. D. A. Saldaña and F. Temelli, *LWT–Food Sci. Technol.*, 2011, **44**, 1880–1887.

